Dynamics of unstable systems

H. A. Posch
Institut für Experimentalphysik, Universität Wien, Boltzmanngasse 5, A-1090 Wien, Austria

H. Narnhofer and W. Thirring
Institut für Theoretische Physik, Universität Wien, Boltzmanngasse 5, A-1090 Wien, Austria
(Received 19 March 1990)

We study the dynamics of classical particles interacting with attractive Gaussian potentials. This system is thermodynamically not stable and exhibits negative specific heat. The results of the computer simulation of the dynamics are discussed in comparison with various theories. In particular, we find that the condensed phase is a stationary solution of the Vlasov equation, but the Vlasov dynamics cannot describe the collapse.

I. INTRODUCTION

There is a widespread feeling that the dynamics of N particles interacting via two-body potentials determined by a Hamiltonian

$$H_N=\frac{1}{2m}\sum_{i=1}^{N}\mathbf{p}_i^2+\sum_i\sum_{j(>i)}\phi_{ij}(\mathbf{x}_i-\mathbf{x}_j) \tag{1.1}$$

reflects the features one learns in kinetic theory. The momentum distribution should become Maxwellian and temperature differences should diffuse away. Finally in equilibrium a distribution homogeneous in $\mathbf{x}$ and Gaussian in $\mathbf{p}$ should be reached, which corresponds to a stationary solution of the Boltzmann equation. Recent[1,2] computer studies have shown that this does not happen generically but on the contrary, if one starts with such a distribution, a cluster can develop and the temperature increases. Only for stable potentials the motion shows the expected features. Stable potentials are such that there exists a constant E_0 such that

$$H_N-E_0N\geq 0 \quad \forall N\ . \tag{1.2}$$

Clearly, if $\phi_{ij}(\mathbf{x}_i-\mathbf{x}_j)=v(\mathbf{x}_i-\mathbf{x}_j)\leq 0 \quad \forall \mathbf{x}_i$, it is not stable. But also an electrostatic type of potential with repulsion and attraction may or may not be stable. If $\phi_{ij}(\mathbf{x}_i-\mathbf{x}_j)=e_ie_jv(\mathbf{x}_i-\mathbf{x}_j)$, $|e_i|=e$, then the potential is stable if $v(\mathbf{x})=e^{-\mathbf{x}^2}$, and unstable if $v(\mathbf{x})=\mathbf{x}^2e^{-\mathbf{x}^2}$. Thus stable potentials are rather special. For unstable potentials also thermodynamic stability gets lost: in a certain energy range the microcanonical specific heat will become negative. This means that the temperature increases with decreasing energy. (Microcanonically the temperature is defined by thermal contact with a small thermometer whereas the canonical temperature corresponds to contact with a big reservoir.[4]) This phenomenon can be understood as follows. Below a certain condensation point a cluster will be formed. In the unstable situation the potential energy per particle and therefore also its kinetic energy will increase with the number of particles in the cluster N_c. Since N_c will increase with decreasing energy so will the kinetic energy of particles giving an increase in temperature with decreasing energy. The thermodynamics of this phenomenon has been analyzed on various theoretical models[3-5] but then it was objected[6] that for these systems the foundations of thermodynamics do not apply and the problem was a dynamical one.

In this paper we report on computer solutions of the equations of motion resulting from (1.1) showing that the dynamical behavior reflects the properties of the thermodynamical picture. In the latter a phase transition occurs between a homogeneous phase and a phase where a small cluster contains a good fraction of all particles. This formation of a dense cluster also happens if the equations of motion are solved on a computer, a phenomenon resembling very much the formation of a star from a cloud of gas. That thermostatics has some bearing on the dynamics has the following origin. The former shows that for $N\to\infty$ the major part of the energy shell corresponds to a big cluster and some atmosphere around it. Thus any orbit will almost surely end up in such a configuration. Although the recurrence theorem applies to such systems and in the exact dynamics such clusters should eventually dissolve again, they do not do so on the computer since the minimal randomness due to roundoff errors prevent strict reversibility. We see in this feature a virtue and not a fault since in real systems one can never completely eliminate all outside influences.

It turns out that the computer solution of the dynamics shows in addition some important effects which are not contained in the thermodynamical description. In this sense there was some truth in the objection put forward in Ref. 6. We find that the heating is such that first the cluster heats up and only eventually the surrounding assumes the same temperature. From the point of view of statistical mechanics this constitutes only a transient phenomenon, but for us who live on the temperature difference of the sun and the earth this is of vital importance. It answers the question how the universe got out of the equilibrium it was supposed to be in originally. If we expand a gas of particles with unstable interactions we

find that at a certain point inhomogeneities in temperature will develop.

II. MICROCANONICAL STATE

In this section we shall study the probability measure $\delta(H_N-E)e^{-S(E)}$ in phase space. We take the latter to be $V^N\times\mathbb{R}^{2N}$ where $V\subset\mathbb{R}^2$ is some finite region the area of which we shall also denote by V. A point in the N-particle configuration space V^N will be written as $\mathbf{X}=(\mathbf{x}_1,\mathbf{x}_2,\ldots,\mathbf{x}_N)$ such that the Hamiltonian assumes the form

$$H_N=\sum_{i=1}^{N}\frac{\mathbf{p}_i^2}{2m}+\Phi(\mathbf{X}),\quad \Phi(\mathbf{X})=-\sum_{j}\sum_{i(>j)}\kappa v(\mathbf{x}_i,\mathbf{x}_j)\ . \tag{2.1}$$

For the pair potential v we shall consider three models: (a),

$$v(\mathbf{x},\mathbf{y})=e^{-|\mathbf{x}-\mathbf{y}|^2/\sigma^2}\ ; \tag{2.2a}$$

(b),

$$v(\mathbf{x},\mathbf{y})=\sum_j \chi_{V_j}(\mathbf{x})\chi_{V_j}(\mathbf{y})\ , \tag{2.2b}$$

where the V_j are a partition of V,

$$\cup_j V_j=V,\quad V_i\cap V_j=\delta_{ij}V_j\ ,$$

and the characteristic function $\chi_{V_j}(\mathbf{x})$ is unity, if $\mathbf{x}\in V_j$ and zero otherwise; and (c),

$$v(\mathbf{x},\mathbf{y})=\chi_{V_0}(\mathbf{x})\chi_{V_0}(\mathbf{y}),\quad V_0\subset V\ . \tag{2.2c}$$

Reduced units are used for which $m=1$ and $\sigma=1$.

Some remarks are worth mentioning.

(1) The essential feature of $\Phi(\mathbf{X})$ is that all the particles attract each other. Though we think about gravity we take in (a) a regular short-range potential to demonstrate that it is neither the singularity nor the long range of the $1/r$ potential which leads to the unusual behavior we are interested in. (b) is a discretization which allows an exact analysis of the partition function.[5] Since it turns out that the system tends to form one big cluster, even the simple version (c) reflects already the salient features.[4]

(2) The usual thermodynamic limit $N\to\infty$ with $\rho=N/V$ and $\varepsilon=E/V$ kept fixed together with the potential strength κ does not exist. However, if we keep $\varepsilon=E/N^2$ as well as V and the potential strength fixed then the entropy per particle, namely, $\lim_{N\to\infty}(1/N)S(\varepsilon N^2,V)$, exists.

First, we calculate the probability density $\rho(\mathbf{X})$ in the configuration space V^N by integrating over the momenta

$$\rho(\mathbf{X})=\int_{-\infty}^{\infty}d^2p_1\cdots d^2p_N\delta(H_N-E)e^{-S(E)}$$
$$=\frac{2^N\pi^N}{(N-1)!}e^{-S(E)}[E-\Phi(\mathbf{X})]^{N-1}\ . \tag{2.3}$$

$\rho(\mathbf{X})$ increases sharply with $|\Phi|$ and since Φ maps V^N onto $[-N(N-1)/2,0]$, points in V^N with many particles close together have a high probability. In (a) $-N(N-1)/2$ is attained if all particles sit on the same point [in the same V_j in (b) or in V_0 in (c)]. On the other hand, these regions have a small volume in configuration space and it is entropically not favorable to put all particles in one big cluster. To estimate the best compromise, consider $N_c<N$ particles in a volume $V_0\subset V$ such that Φ is $\sim N_c^2\gg E$. This configuration has a probability

$$P_1\sim\left[\frac{V_0}{V}\right]^{N_c-1}(N_c^2)^{N-1}\ ,$$

which attains its maximum for $N_c\sim 2N/\ln(V/V_0)$. Two clusters of half the size have a probability

$$P_2\sim\left[\frac{N_c}{N_c/2}\right]\left[\frac{V_0}{V}\right]^{N_c-2}\left[\left[\frac{N_c}{2}\right]^2\right]^{N-1}$$
$$\sim P_1\frac{V}{V_0}2^{-N}\ .$$

Thus for V_0 fixed and $V\sim N$ it is advantageous to make one big cluster. These rough arguments can be made exact in model (c). With N_c as the number of particles in V_0 define

$$e^S=V_0^N\frac{2^N\pi^N}{(N-1)!}\sum_{N_c=0}^{N}\left[\frac{V}{V_0}-1\right]^{N-N_c}\frac{(E+N_c^2/2)^{N-1}N!}{N_c!(N-N_c)!}\equiv N!\sum_{N_c=0}^{N}e^{N\sigma(N_c/N)}\ . \tag{2.4}$$

If we take the limit $N\to\infty$ with $\varepsilon=2E/N^2$ and V/V_0 fixed we find with $\alpha=N_c/N$:

$$\sigma(\alpha)=\ln(\varepsilon+\alpha^2)-\alpha\ln\alpha-(1-\alpha)\ln(1-\alpha)+(1-\alpha)\ln\left[\frac{V}{V_0}-1\right]+\text{const.} \tag{2.5}$$

The maximum is attained if

$$\varepsilon=-\alpha^2+\frac{2\alpha}{\ln\left[\frac{V}{V_0}-1\right]-\ln\left[\frac{1}{\alpha}-1\right]}\ , \tag{2.6}$$

which gives for $V/V_0\gg 1$ and $\varepsilon\to 0$ the previous estimate for N_c.

If we compare N_c with our computer simulation in Sec. V, then V_0 has to be chosen of the order of the range of v. Thus $V/V_0\sim 800$ and $N=400$. With these values about $\frac{1}{3}$ of the particles will be concentrated in V_0, in qualitative agreement with the simulation.[1,2]

Next we turn to the question of the local temperature and define a map T: $V^N \to \mathbb{R}^+$ by

$$T(\mathbf{X}) = \int_{-\infty}^{\infty} d^2p_1 \cdots d^2p_N \frac{\mathbf{p}_1^2}{2} \delta(E - H_N) e^{-S(E)}$$

$$= \left\langle \frac{\mathbf{p}_i^2}{2} \right\rangle_{\mathbf{X}} \tag{2.7}$$

such that the local temperature is just the expectation value of the kinetic energy of a single particle at a given point $\mathbf{X}$ in configuration space.

At this stage some comments are in order.

(1) At a given point $\mathbf{X} \in V^N$ the distribution is the same for all $\mathbf{p}_i$ [we could have integrated $(1/N)\sum \mathbf{p}_i^2$ instead of $\mathbf{p}_1^2$]. This means that in equilibrium the particles outside the cluster are just as hot as the ones inside.

(2) The microcanonical state differs from the canonical state by the $\mathbf{X}$ dependence of T. If we replace $\delta(H_N - E)e^{-S(E)}$ by $e^{-\beta[H_N - F(\beta)]}$ then $T = 1/\beta$ irrespective of $\mathbf{X}$. F is the free energy. Of course, in the translation-invariant model (a) T depends only on the correlations between the particles and $V^{N-1}\int d^2x_2 \cdots d^2x_N T(\mathbf{X})$ becomes independent of $\mathbf{x}$ and in the limit $N \to \infty$ the microcanonical temperature $[\partial S(E)/\partial E]^{-1}$.

(3) It has to be remembered that $T(\mathbf{X})$ is the temperature for the configuration $\mathbf{X}$ in the equilibrium state. In the dynamical studies the following transient features appear. If a cluster with N_c particles is formed then locally the gain both in potential and in kinetic energy is $\sim N_c^2$. Thus in the cluster the system heats up to a temperature $\sim N_c$. However, the cluster is not thermally insulated, and eventually its temperature is distributed over all particles to give a common equilibrium temperature $\sim N_c^2/N$ (compare Sec. VI).

With the Hamiltonian (2.1) we calculate ($m = 1$)

$$T(\mathbf{X}) = \frac{1}{N}[E - \Phi(\mathbf{X})] \, . \tag{2.8}$$

We note the following.

(1) Since $-\Phi \sim N_c^2$ we get $T \sim N_c^2/N$ as soon as $E \ll N_c^2$, for instance, if we start with $E \sim N$ and $N_c \sim N/3$.

(2) The definition (2.7) gives an $\mathbf{X}$-dependent temperature even for thermodynamically stable systems. However, if $\Phi(\mathbf{X}) > -cN$ and $E \sim N$ there will be only fluctuations around

$$T = \frac{1}{N}\left[E - \int d^2x_1 \cdots d^2x_N \Phi(\mathbf{X})\right] .$$

To justify the definition (2.7) we have to inspect whether the momenta are actually distributed according to a Maxwell-Boltzmann distribution for given $\mathbf{X} \in V^N$. For that we calculate the conditional probability

$$\rho(\mathbf{X}, \mathbf{p}_1) = \frac{1}{\rho(\mathbf{X})} \int d^2p_2 \cdots d^2p_N \delta(H_N - E) e^{-S(E)}$$

$$= \left[E - \Phi(\mathbf{X}) - \frac{\mathbf{p}_1^2}{2}\right]^{N-2}$$

$$\times \frac{(N-1)\Theta(E - \Phi(\mathbf{X}) - \mathbf{p}_1^2/2)}{2\pi[E - \Phi(\mathbf{X})]^{N-1}} \, .$$

As $(1 - a/N)^N \to e^{-a}$ we see that for large N the distribution approaches $C(\mathbf{X})e^{-\mathbf{p}_1^2/2T(\mathbf{X})}$. This is verified by our simulation results in Sec. VI.

III. CANONICAL STATE

The thermodynamic functions and states have been calculated in the limit $N \to \infty$ explicitly for the models (b) and (c).[4,5,1] One finds that for small energies the phase space is dominated by a configuration with one cluster containing a finite fraction of all particles. These calculations have been generalized in Refs. 7 and 8 to the more realistic situation of the gravitational $1/r$ potential. There one needs quantum theory to mollify the singularity but, in principle, the analysis reduces the problem to one of type (b). Dividing the volume into a large but finite number of cells with constant potentials determined self-consistently one can approximate the full problem such that in the limit $N \to \infty$ the relative error goes to zero. We do not want to repeat this lengthy demonstration here since it is clear that it also works in the present setting. Instead we shall give a simpler derivation of the mean-field theory without proving the finer details of rigor.

We consider N particles in a fixed d-dimensional volume V. The canonical density in phase space

$$\rho_N(\mathbf{x}_1, \ldots, \mathbf{p}_N) = \exp\left[-\beta\left(\sum_{i=1}^{N} \frac{\mathbf{p}_i^2}{2} - \kappa \sum_{i,j} v(\mathbf{x}_i - \mathbf{x}_j) - F(\beta)\right)\right] \tag{3.1}$$

is characterized by the fact that it maximizes the entropy. For a density $\bar{\rho}$ the latter is defined by

$$S(\bar{\rho}_N) = -\int d\Omega \, \bar{\rho} \ln \bar{\rho}, \quad d\Omega = d^2x_1 \cdots d^2p_N \, . \tag{3.2}$$

For fixed expectation value of the energy,

$$E_N = \int d\Omega \rho_N H_N = \int d\Omega \bar{\rho}_N H_N \, , \tag{3.3}$$

we have $S(\rho_N) \geq S(\bar{\rho}_N)$. E_N is the sum of the kinetic energy

$$K = N \int d^2x \, d^2p \frac{\mathbf{p}^2}{2} \rho_N^{(1)}(\mathbf{x}, \mathbf{p}) \tag{3.4}$$

and the potential energy

$$\Phi = -\kappa \frac{N(N-1)}{2} \int d^2x_1 d^2x_2 d^2p_1 d^2p_2 \times \rho_N^{(2)}(\mathbf{x}_1, \mathbf{x}_2, \mathbf{p}_1, \mathbf{p}_2) v(\mathbf{x}_1 - \mathbf{x}_2) \, , \tag{3.5}$$

where we have introduced the k-particle distributions

$$\rho_N^{(k)}(\mathbf{x}_1,\ldots,\mathbf{p}_k) = \int \rho_N(\mathbf{x}_1,\ldots,\mathbf{p}_N) d^2x_{k+1}\cdots d^2p_N \ . \tag{3.6}$$

Since $\Phi \sim N^2$ we also want $K \sim N^2$ which requires a scaling such that for $N\to\infty$, V fixed, the limit

$$\lim_{N\to\infty} N^k \rho_N^{(k)}(\mathbf{x}_1,\ldots,\mathbf{x}_k;\sqrt{N}\,\mathbf{p}_1,\ldots,\sqrt{N}\,\mathbf{p}_k) = \tilde{\rho}^{(k)}(\mathbf{x}_1,\ldots,\mathbf{p}_k) \tag{3.7}$$

exists. Then

$$\varepsilon \equiv \lim_{N\to\infty} N^{-2}(K+\Phi) = \int d^2x\, d^2p\, \tilde{\rho}^{(1)}(\mathbf{x},\mathbf{p})\frac{\mathbf{p}^2}{2} - \frac{\kappa}{2}\int d^2x_1\cdots d^2p_2 \tilde{\rho}^{(2)}(\mathbf{x}_1,\ldots,\mathbf{p}_2) v(\mathbf{x}_1-\mathbf{x}_2) \ . \tag{3.8}$$

So far we have no relation between $\tilde{\rho}^{(1)}$ and $\tilde{\rho}^{(2)}$ but we may use the result of Ref. 9 that any symmetrical density $\tilde{\rho}^{(k)}(\mathbf{x}_1,\ldots,\mathbf{p}_k)$ can be approximated arbitrarily closely by (finite) convex combinations of product densities

$$\tilde{\rho}^{(k)}(\mathbf{x}_1,\ldots,\mathbf{p}_k) = \sum_j \alpha_j \prod_{i=1}^{k} \hat{\rho}_j(\mathbf{x}_i,\mathbf{p}_i) \ . \tag{3.9}$$

The deeper part of this theorem is that we can take all $\alpha_j > 0$ and—if the $\hat{\rho}_j$ are normalized according to $\int \hat{\rho}_j(\mathbf{x}_i,\mathbf{p}_i) d^2x_i d^2p_i = 1$—we have $\sum_j \alpha_j = 1$.

The energy is then the convex combination

$$\varepsilon = \sum_j \alpha_j \left[\int d^2x\, d^2p\, \hat{\rho}_j(\mathbf{x},\mathbf{p})\frac{\mathbf{p}^2}{2} - \frac{\kappa}{2}\int d^2x_1\cdots d^2p_2 v(\mathbf{x}_1-\mathbf{x}_2)\hat{\rho}_j(\mathbf{x}_1,\mathbf{p}_1)\hat{\rho}_j(\mathbf{x}_2,\mathbf{p}_2) \right] . \tag{3.10}$$

The entropy for a product density is simply additive,

$$S\left[\prod_{i=1}^{N}\rho(\mathbf{x}_i,\mathbf{p}_i)\right] = NS(\rho) \ . \tag{3.11}$$

Furthermore, S is concave but not too concave in the sense that one has the general inequalities with the mixing entropy

$$\sum_j \alpha_j S(\bar{\rho}_j) \le S\left[\sum_j \alpha_j \bar{\rho}_j\right] \le \sum_j \alpha_j S(\bar{\rho}_j) - \sum_j \alpha_j \ln\alpha_j \ . \tag{3.12}$$

We shall apply these inequalities to the case where the $\bar{\rho}_j$ is the product of the densities $\hat{\rho}_j$ for the individual particles. Dividing (3.12) by N and passing to the limit $N\to\infty$ we find

$$\lim_{N\to\infty}\frac{1}{N}S(\rho_N) = \sum_j \alpha_j S(\hat{\rho}_j) \tag{3.13}$$

provided we can exchange this limit with the convex combinations such that $(1/N)\sum_j \alpha_j \ln\alpha_j = 0$. Up to this point everything we said was rigorous but here we have to refer to the literature for justifying this assumption. Since the entropy (3.13) and ε (3.10) are the same convex combinations of contributions of the individual $\hat{\rho}_j$ it is clear that the maximum of S for given ε is reached by taking the best $\hat{\rho}_j$. The corresponding variational equations require

$$-\ln\rho(\mathbf{x},\mathbf{p}) = \beta\left[\frac{\mathbf{p}^2}{2} - \kappa\int v(\mathbf{x}-\mathbf{y})\rho(\mathbf{y},\mathbf{q}) d^2y\, d^2q\right] + \nu_0 \ .$$

Here β and ν_0 are Lagrange multipliers, the latter ensuring $\int d^2x\, d^2p\, \rho(\mathbf{x},\mathbf{p}) = 1$. Thus ρ has the barometric form

$$\rho(\mathbf{x},\mathbf{p}) = e^{-\beta\mathbf{p}^2/2 + \nu(\mathbf{x}) - \nu_0} \tag{3.14}$$

where $\nu(\mathbf{x})$ is determined by the self-consistency equation

$$\nu(\mathbf{x}) = \beta\kappa \int v(\mathbf{x}-\mathbf{y}) e^{\nu(\mathbf{y})} d^2y \Big/ \int d^2y\, e^{\nu(\mathbf{y})} \ . \tag{3.15}$$

We shall now return to our case of interest where the particles move on a torus, $V = T^2$. It is clear that (3.15) always has the constant solution $\nu(\mathbf{x}) = \beta\kappa\int d^2y\, v(\mathbf{y})/V$. In fact, an expansion in powers of κ leads only to the constant solution. The nonperturbative character of a nonconstant solution is illustrated by

Proposition. Let v: $T^2 \to \mathbb{R}^+$ be such that $i \le v(\mathbf{x}) \le s$, $\int d^2x\, v(\mathbf{x}) = 1$ where d^2x is the normalized volume element on T^2 ($\int_{T^2} d^2x = 1$). Then the integral equation

$$\nu(\mathbf{x}) = b\frac{\int d^2y\, v(\mathbf{x}-\mathbf{y}) e^{\nu(\mathbf{y})}}{\int d^2y\, e^{\nu(\mathbf{y})}}$$

has for $b < [1/(s-i)]\operatorname{arcsinh}[(s-i/2)]$ only the constant solution $\nu(\mathbf{x}) = b$.

Proof. Denote by $\nu_{1,2}$ the bounds of ν, $\nu_1 \le \nu(\mathbf{x}) \le \nu_2$. Then $\nu_2 \le be^{\nu_2-\nu_1}$, $\nu_1 \ge be^{\nu_1-\nu_2}$ or if $g = \nu_2 - \nu_1$, $g \le b(e^g - e^{-g})$. For $b < \frac{1}{2}$ this equation is satisfied only for $g = 0$ or $g \ge$ some $g_0(b)$, $g_0' < 0$. From the variation of v we know $|\nu(\mathbf{x}) - \nu(\mathbf{x}')| \le b(s-i)$ or $g \le b(s-i)$. The condition $g_0(b) = b(s-i)$ implies $b(s-i) = 2b\sinh[b(s-i)]$, which yields the quoted bound for b.

Since b in our case is the ratio between the strength κ of the potential and the temperature, this proposition tells us that only for sufficiently strong attraction can a cluster develop. That this actually happens follows from the fact that in this case the one-particle entropy for a $\rho^{(1)}(\mathbf{x},\mathbf{p})$ clustering in $\mathbf{x}$ is higher than for a homogeneous distribution with the same ε. The reason is that one gains so much potential energy that ρ is all the more spread out

in $\mathbf{p}$. For a distribution which factors in $\mathbf{x}$ and $\mathbf{p}$ the entropy is simply the sum of the log of the volumes in $\mathbf{x}$ and $\mathbf{p}$ over which ρ is smeared out. With the approximate N scaling we have $\varepsilon=(\mathbf{p}^2/2)-\kappa$ with a cluster and $\varepsilon=\mathbf{p}^2/2$ without a cluster. Thus the difference between the entropies of a clustering and a homogeneous distribution is $\ln V_0/V+\ln(\varepsilon+\kappa)/\varepsilon$ and ε is positive and sufficiently small. This also proves that for large κ (3.15) must have a nonconstant solution since—taking the necessary continuity for granted—the one-particle entropy has to attain its maximum, and this cannot be for constant $\nu(\mathbf{x})$.

Equations (3.14) and (3.15) are numerically solved in Sec. VII and the results are compared to the simulation.

IV. TIME EVOLUTION

So far we have seen that the equilibrium thermostatics is described by a mean-field theory. There exists a counterpart to that for the time evolution, namely, the Vlasov dynamics. In Refs. 10 and 11 it is shown that in the limit $N\to\infty$ the time evolution due to a Hamiltonian

$$H_N=\sum_{i=1}^{N}\frac{\mathbf{p}_i^2}{2}-\kappa\sum\sum v(\mathbf{x}_i-\mathbf{x}_j)$$

is described by the Vlasov dynamics if the particles stay in a fixed volume V. In our scaling procedure these results imply that

$$\rho(\mathbf{x},\mathbf{p},t)=\lim_{N\to\infty}N\rho_N^{(1)}(\mathbf{x},\mathbf{p}\sqrt{N},t/\sqrt{N})$$

satisfies the Vlasov equation for

$$\frac{\partial\rho(\mathbf{x},\mathbf{p},t)}{\partial t}=\mathbf{p}\frac{\partial\rho(\mathbf{x},\mathbf{p},t)}{\partial x}+\frac{\partial\rho(\mathbf{x},\mathbf{p},t)}{\partial\mathbf{p}}\kappa\int\nabla v(\mathbf{x}-\mathbf{y})\rho(\mathbf{y},\mathbf{q},t)d^2y\,d^2q\ . \tag{4.1}$$

Therefore the time scale for which the Vlasov dynamics is correct is the time in which particles move a finite distance in the fixed volume. However, in the limit $N\to\infty$ the velocities increase so much that this time becomes negligibly small and (4.1) does not describe how a cluster develops. That it is incapable of doing this is a consequence of Liouville's theorem since the Vlasov dynamics is governed by a one-parameter family of canonical transformations $(\mathbf{x},\mathbf{p})\to(\mathbf{x}(t),\mathbf{p}(t))$, $\rho(\mathbf{x},\mathbf{p},t)=\rho(\mathbf{x}(t),\mathbf{p}(t),0)$ determined by

$$\frac{d\mathbf{x}(t)}{dt}=\mathbf{p}(t)\ ,\qquad \frac{d\mathbf{p}(t)}{dt}=\kappa\int\nabla v(\mathbf{x}-\mathbf{y})\rho(\mathbf{y},\mathbf{q},t)d^2y\,d^2q\ . \tag{4.2}$$

As a consequence all p norms $\|\rho\|_p=[\int d^2x\,d^2q\,\rho^p(\mathbf{x},\mathbf{q},t)]^{1/p}$ are t independent and so is the one-particle entropy (a generalized Gibb paradox)

$$S=-\int d^2x\,d^2p\,\rho(\mathbf{x},\mathbf{p},t)\ln\rho(\mathbf{x},\mathbf{p},t)=\lim_{p\to1}\frac{p}{1-p}\ln\|\rho\|_p\ . \tag{4.3}$$

Thus (4.1) cannot describe the evolution of a homogeneous density $\rho(\mathbf{x},\mathbf{p})=ce^{-\beta\mathbf{p}^2/2}$ to a clustered one since we have seen that the latter has a higher entropy. Nevertheless, the equilibrium density ought to satisfy (4.1) since a constant density does not change even in a short time. Indeed (3.14) and (3.15) describe just a time-independent solution of (4.1). However, it is by no means the only stationary solution of this equation. According to (4.2) any function depending only on the constants of motion will be time independent. Thus with an ansatz of any function f of the energy,

$$\rho(\mathbf{x},\mathbf{p})=f\left[\frac{\mathbf{p}^2}{2}-\nu(\mathbf{x})\right],$$

one can solve (4.1) provided the potential ν is determined by the self-consistency equation

$$\nu(\mathbf{x})=\int v(\mathbf{x}-\mathbf{y})f\left[\frac{\mathbf{p}^2}{2}-\nu(\mathbf{y})\right]d^2y\,d^2p \tag{4.4}$$

in agreement with (3.15).

We note the following.

(1) One might hope that the final equilibrium state is approached via stationary solutions of the Vlasov equation. The computer studies reveal that first the cluster heats up and just eventually gets into equilibrium with the rest. Thus one might look for solutions which have the property that

$$\int d^2p\,\mathbf{p}^2f(\mathbf{p}^2/2-\nu)\Big/\int d^2p\,f(\mathbf{p}^2/2-\nu)$$

is an increasing function with ν. One easily sees this happen if $\ln f$ is a concave function. However, nothing else distinguishes these solutions and one cannot say that this feature is predicted by the Vlasov equation.

(2) The stationary solutions are not attractors for the Vlasov dynamics. If ρ is of the form $\rho_0(\mathbf{x},\mathbf{p})+\rho_1(\mathbf{x},\mathbf{p},t)$, then also $\rho_1(\mathbf{x},\mathbf{p},t)=\rho_1(\mathbf{x}(t),\mathbf{p}(t),0)$ and all p norms of ρ_1 are constant. However, if ρ_0 is normalized, then $\int d^2x\,d^2p\,\rho_1(\mathbf{x},\mathbf{p},t)=0$ and it is possible that ρ_1 goes to zero in the mean. In particular, if $\rho_1\ll\rho_0$, $\mathbf{x}(t)$ and $\mathbf{p}(t)$ are determined essentially by ρ_0 and therefore a time-independent Hamiltonian. If the latter leads to a mixing motion, the ρ_1 will weakly go to zero and ρ_0 is a weak attractor.

V. SIMULATION OF CLUSTER FORMATION

As a test of these theoretical considerations we have carried out a series of computer simulations which are presented in this and the following sections. They are based on the smooth and purely attractive pair potential of model (2.2a). The first simulations of such a system have been carried out recently by Compagner, Bruin, and Roelse.[1] Concentrating on the equilibrium properties they have shown that the qualitative features of the microcanonical cell model (2.2b) are well reproduced by the simulation results for equilibrium states of model (2.2a). This is verified also by our computations, a first account of which is given in Ref. 2. In the following we shall be

TABLE I. Equilibrium properties for various simulation runs. e and Θ are energy and temperature parameters defined in (5.3) and (5.4), respectively, and $N_c(\infty)$ is the number of particles in the cluster. For all runs $N=400$. (a) and (b) indicate the type of initial conditions used as explained in Sec. V. The statistical error for Θ is about 3%. The symbols G and C refer to gaseous and clustered states, respectively, and E denotes a system of charged particles discussed in Sec. IX.

Run	N/V	Initial condition	e	Θ	$N_c(\infty)$
C1	0.5	(a)	0.9226	0.113	210
C2	0.5	(a)	1.0009	0.083	142
C3	0.5	(a)	1.0059	0.081	140
C4	0.5	(b)	1.0060	0.079	142
G1	0.5	(a)	1.0593	0.063	
C5	0.125	(a)	1.0060	0.054	~100
G2	0.125	(a)	1.0593	0.060	
E1	0.5	(a)	1.0028	0.012	128

mainly concerned with transient states leading from nonequilibrium initial states to equilibrium.

The Hamiltonian of model (2.2a) is given by

$$H_N=\sum_{i=1}^{N}\frac{\mathbf{p}_i^2}{2m}-\kappa\sum_{i=1}^{N-1}\sum_{j=i+1}^{N}v(\mathbf{x}_i-\mathbf{x}_j) \tag{5.1}$$

$$v(\mathbf{x}-\mathbf{y})=e^{-(\mathbf{x}-\mathbf{y})^2/\sigma^2},\quad \kappa>0\ , \tag{5.2}$$

and, as before, reduced units are used, for which the particle mass m, the strength κ of the potential and the range parameter σ are unity. The simulations are performed on a two-dimensional torus and with $N=400$ particles. A Gear predictor-corrector algorithm in the N representation and correct through terms of order Δt^3 is employed[12] with a time step $\Delta t=0.0025$ for most of the runs.

Two different types of initial conditions are used: (a) All N particles are distributed randomly over the square torus T^2 with volume $V=L^2$; (b) All N particles are in a perfect cluster and on top of each other. In both cases the velocity components v_α are taken as equally distributed in $-v_0<v_\alpha<v_0$, $v_0=[3K(0)/Nm]^{1/2}$, and $K(0)$ is the initial kinetic energy. For initial condition (a) and low enough energy E, small clusters are immediately formed after initiating the simulation. Typically one of these clusters grows fast and dominates the rest by accepting more and more particles until it finally reaches its equilibrium particle number $N_c(\infty)$. This number may amount to $N/3$ or more depending primarily on the ratio L/σ (Sec. II). The simultaneous growth of a second large cluster usually is suppressed. We shall come back to this point in Sec. IX. For initial condition (b) the initial potential energy is strongly negative, $\Phi(0)=-N(N-1)/2$. Consequently, for the same E as before $K(0)$ has to be very large and the initially perfect cluster disintegrates quickly by boiling off particles into the atmosphere. It finally approaches the *same* $N_c(\infty)$ as for (a). In both cases the approach to equilibrium is very slow. Typically more than 3 million time steps are required as will be discussed further in Sec. VIII. The energy E is conserved by the microcanonical simulation to better than 0.2% over the whole length of the run.

For the characterization of the final equilibrium states we define energy and temperature parameters by

$$e=1+\frac{2E}{N(N-1)\kappa}\ , \tag{5.3}$$

$$\Theta=\frac{4K(\infty)}{dN^2\kappa}=\frac{2k_BT(\infty)}{N\kappa}\ , \tag{5.4}$$

where the dimension $d=2$. $T(\infty)$ is the equilibrium temperature and k_B Boltzmann's constant (set to unity as in previous sections). The relevant thermodynamic properties for the various simulated states are collected in Table I. States G1 and G2 (G denotes gas) have an energy $e>e_t$, the transition energy, and are incapable of forming a large cluster. They behave as an ideal gas with positive specific heat. For states labeled C1–C5 (C denotes cluster) we have $e<e_t$, and a cluster is formed. Since $d\Theta(e)/de<0$ in this e range the respective specific heat is negative. The transition energy e_t is very close but not identical to unity. For details of the equilibrium properties and the phase diagram $\Theta(e)$, Refs. 1, 2, 4, and 5 should be consulted.

VI. TEMPERATURE OF TRANSIENT CLUSTERS

The definition of a cluster is somewhat arbitrary, but it turns out that its properties are insensitive to the particular definition. We take the inflection point of the potential (5.2), $D=\sigma/\sqrt{2}$, as the defining interaction range: two particles i,j are said to belong to the same cluster if $|\mathbf{x}_i-\mathbf{x}_j|<D$. During the simulation a complete cluster analysis is performed after every 100 time steps. The evaluation of time-dependent averages over a nonequilibrium ensemble of trajectories is prohibitively expensive. We have therefore compromised by averaging dynamical variables over phase configurations with a given cluster particle number N_c' realized by a single trajectory (Fig. 1). Since the time-smoothed value $\bar{N}_c$ changes slowly in the course of the simulation (Sec. VIII), an average over configurations associated with the large dots in Fig. 1 yields what may be viewed as a nonequilibrium average at time t'. It is denoted by $\langle\ldots;N_c'\rangle$. From this definition it is obvious that the number of configurations sampled with a particular N_c'—and therefore the statistical uncertainty of the average—depends on the rate of change of $\bar{N}_c$. This rate is reflected in the length of the error bars in

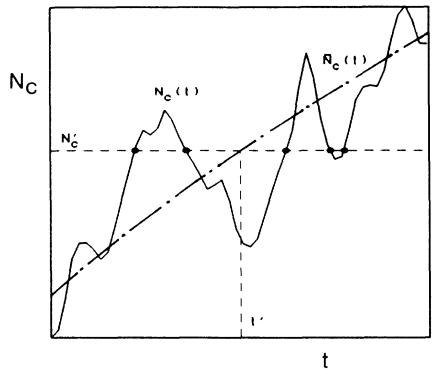

FIG. 1. Schematic representation of calculating nonequilibrium averages from a single trajectory. $N_c(t)$ is the fluctuating number of cluster particles and $\bar{N}_c(t)$ is its time-smoothed behavior. During the transient stage all configurations with a given N_c' (as indicated by the dots) contribute to a nonequilibrium average associated with time t' and denoted by $\langle \ldots ; N_c' \rangle$.

Fig. 2, large error bars indicating fast cluster growth. Once equilibrium is established N_c fluctuates around its equilibrium value [$N_c(\infty)=140$ for run C3] and the error bars become very small.

Let us define the peculiar kinetic energy of the main cluster per cluster particle by

$$K_c/N_c=\frac{1}{N_c}\left\langle \sum_{i=1}^{N_c}\frac{m}{2}(\mathbf{v}_i-\mathbf{V}_c)^2;N_c\right\rangle , \tag{6.1}$$

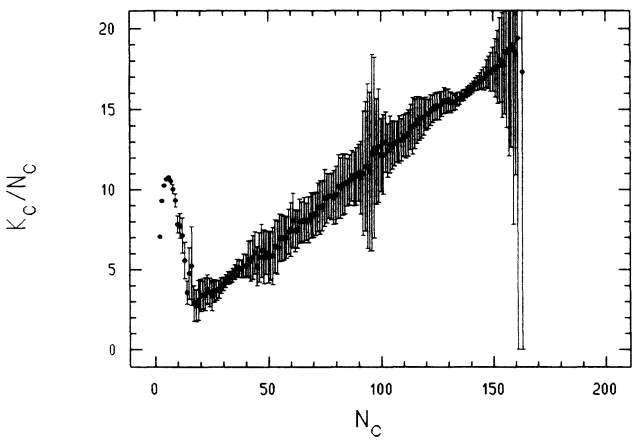

FIG. 2. Peculiar kinetic energy K_c per cluster particle as a function of the cluster-particle number N_c for system C3. The length of the error bars indicates how often a cluster with a given N_c has been sampled during the transient growth stage of the cluster. Once equilibrium is approached N_c fluctuates around 140 accounting for the small error bars. At the beginning of the simulation all $N=400$ particles are equally distributed over the accessible volume $V=400$. The initial total kinetic energy $K=800$ corresponds to a temperature $T=2$. In the collapsing cluster this temperature rises proportional to N_c to reach $T\simeq 16.3$ for equilibrium conditions.

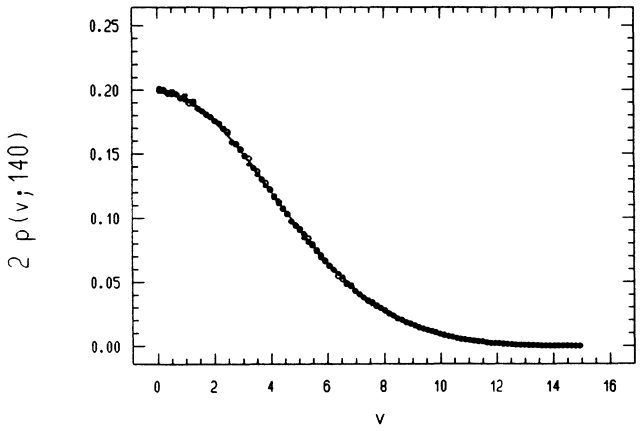

FIG. 3. Normalized velocity distribution of the cluster particles (solid circles) and of the gas particles (open circles) for the final equilibrium state of run C3, for which the cluster particle number N_c fluctuates around 140. The temperature of the gas and of the cluster are equal ($T_g\simeq T_c=16.3$) as predicted by the comments following Eq. (2.7). As required by the comments following Eq. (2.8) the distributions are well represented by Maxwell-Boltzmann distributions (solid lines).

with $\mathbf{v}_i$ the velocity of particle i and $\mathbf{V}_c$ the center-of-mass velocity of the cluster. For state C3 and initial conditions of type (a) this quantity is shown in Fig. 2 as a function of N_c which grows slowly in the course of the simulation. In agreement with the theoretical expectation commented about in (3) following Eq. (2.7), K_c/N_c—and therefore the local cluster temperature—is

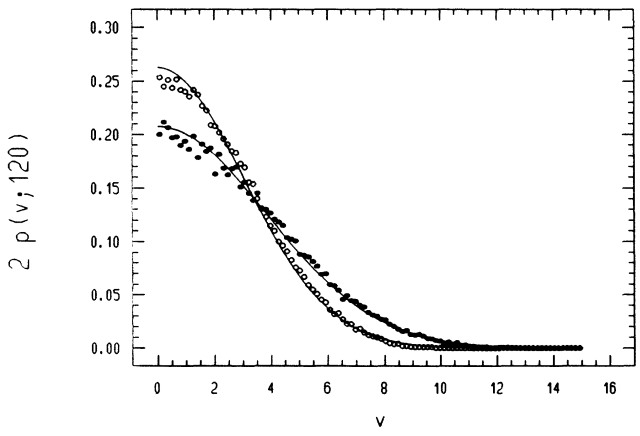

FIG. 4. Normalized velocity distribution of the cluster particles (solid circles) and of the surrounding gas (open circles) for the transient nonequilibrium stage of system C3 with $N_c=120$. The gas distribution is narrower indicating a lower temperature in the gas ($T_g=9.2$) than in the cluster ($T_c=14.7$). The solid curves are calculated from a Maxwell-Boltzmann distribution. During the collapsing stage the number of configurations with a given $N_c=120$ available for averaging is comparatively small, and the statistical noise is therefore larger than in Fig. 3.

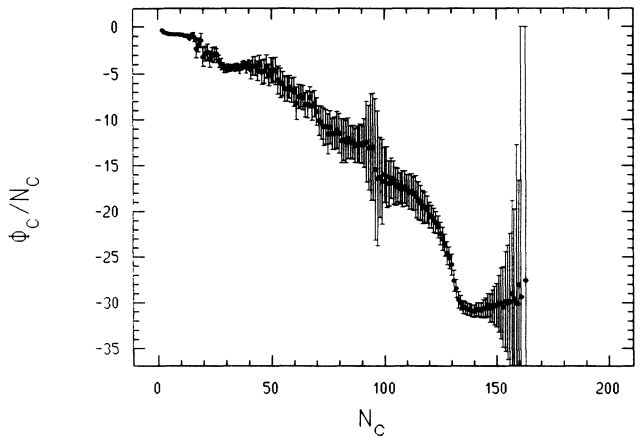

FIG. 5. Potential energy per cluster particle as a function of the cluster-particle number N_c for system C3. During the nonequilibrium growth Φ_c is continuously lowered with growing N_c until equilibrium is reached for $N_c \simeq 140$. As in Fig. 2 the length of the error bars indicates how often a particular N_c has been sampled during the simulation covering the transient stage.

$\sim N_c$ in the transient stage, whereas the surrounding gas remains significantly cooler. Only after reaching equilibrium do the cluster and the gas end up at a common temperature $\sim N_c^2/N$.

In Fig. 3 the normalized velocity distributions of cluster particles (solid circles) and of the surrounding gas (open circles) for conditions close to the equilibrium state of run C3 are shown. Both distributions are practically identical and correspond to a Maxwell-Boltzmann distribution (solid lines) with a temperature $T_g \simeq T_c = 16.3$. The notion of a local temperature is meaningful also for nonequilibrium transient states. For the same run C3 these respective normalized velocity distributions are shown in Fig. 4 for a nonequilibrium state with a cluster number $N_c = 120 < N_c(\infty)$. The distribution for the cluster is broader than that of the gas, and $T_c = 14.7 > T_g = 9.2$. The solid curves are the respective Maxwell-Boltzmann distributions.

The potential energy per cluster particle is defined for a cluster according to

$$\Phi_c/N_c = -\frac{1}{N_c}\left\langle \sum_{i=1}^{N_c-1} \sum_{j=i+1}^{N_c} v(\mathbf{x}_i - \mathbf{x}_j); N_c \right\rangle , \qquad (6.2)$$

where the sums are over all cluster particles. For the growth stage of run C3 this quantity is shown in Fig. 5 as a function of N_c. The previous remarks concerning the length of the error bars also apply to this case.

VII. SIZE OF THE CLUSTER

One of the most noteworthy results is that the size of the cluster is hardly affected by the condensation process during the transient approach to equilibrium. This is demonstrated in Fig. 6 where we plot a parameter s defined by

$$s^2 = \frac{2}{N_c(N_c-1)}\left\langle \sum_{i=1}^{N_c-1} \sum_{j=i+1}^{N_c} (\mathbf{x}_i - \mathbf{x}_j)^2; N_c \right\rangle \qquad (7.1)$$

as a function of N_c for the collapsing regime of run C3. s is the root-mean-square separation of cluster particles over which the sums in (7.1) are performed. For all practical purposes s is a constant and close to $\sigma/3$, $\sigma = 1$. In hindsight this result explains the success of model (2.2c) which assumes a single small subvolume $V_0 \subset V$, in which all the clustering takes place. As already mentioned this model contains all the salient features of the more sophisticated model (2.2b) which introduces a whole partition of V.

The spatial distribution of particles in the system may be studied by defining local particle densities with respect to $\mathbf{R}_c$, the center of mass of the cluster. Putting the ori-

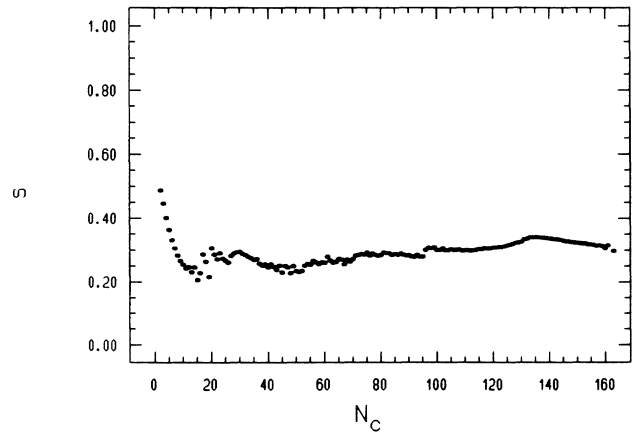

FIG. 6. Average root-mean-square separation s of cluster particles as a function of N_c during the transient condensation process for run C3.

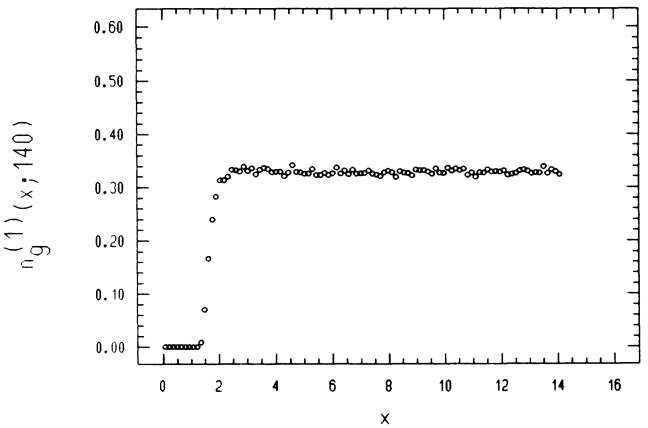

FIG. 7. Local one-particle density $n_g^{(1)}(x;140)$ of the gas for run C3, $(N_c = 140)$ as a function of the separation x from the center of mass $\mathbf{R}_c$ of an equilibrated cluster. The gas is equally distributed over the accessible volume in accord with the prediction of the cell models introduced in Sec. II.

gin of our reference system into $\mathbf{R}_c$ we have for the cluster

$$n_c^{(1)}(x;N_c)=\left\langle \sum_{i=1}^{N_c} \delta(\mathbf{x}-\mathbf{x}_i);N_c \right\rangle , \tag{7.2}$$

$$\int_V n_c^{(1)}(x;N_c)d^2x = N_c , \tag{7.3}$$

and for the gas

$$n_g^{(1)}(x;N_c)=\left\langle \sum_{i\in \text{gas}} \delta(\mathbf{x}-\mathbf{x}_i);N_c \right\rangle , \tag{7.4}$$

$$\int_V n_g^{(1)}(x;N_c)d^2x = N-N_c . \tag{7.5}$$

The sums in (7.2) and (7.4) are over the cluster and gas particles, respectively. Since there is no preferred direction these functions depend only on $x=|\mathbf{x}|$, the scalar separation from $\mathbf{R}_c$.

In Fig. 7 $n_g^{(1)}(x;140)$ is shown for equilibrium conditions of run C3. The gas density is homogeneous thus confirming the theoretical predictions of model (2.2b) and the respective assumptions underlying model (2.2c).

The density profile for the cluster, however, is more interesting. It is depicted in Fig. 8 for the respective equilibrium states of runs C1 and C3. These distributions are bell shaped. We want to compare these results to the predictions of the mean-field theory outlined in Sec. III which is expected to apply to this equilibrium situation. $n_c^{(1)}(x;N_c(\infty))$ is identified with $\rho(\mathbf{x},\mathbf{p})$ in (3.14), integrated over $\mathbf{p}$ and properly renormalized to comply with (7.3):

$$n_c^{(1)}(x;N_c(\infty))\sim \int \rho(x,\mathbf{p})d\mathbf{p} . \tag{7.6}$$

As before, the origin of the coordinate system has been placed in $\mathbf{R}_c$ and both $\rho(x,\mathbf{p})$ and $v(x)$ in(3.15) may depend only on the absolute separation from the origin. To

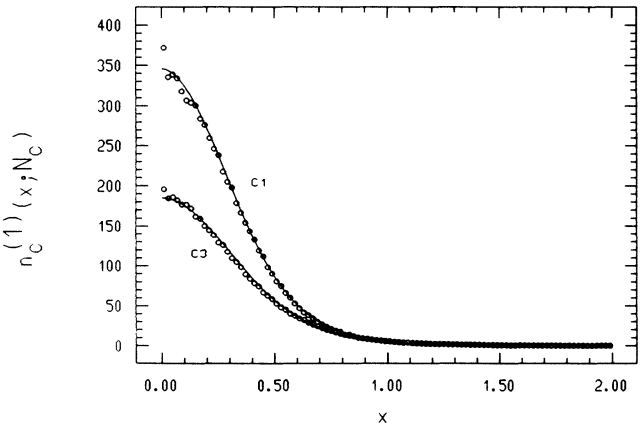

FIG. 8. Local particle density $n_c^{(1)}(x;N_c)$ in the cluster for the two simulation runs C1 ($N_c=210$) and C3 ($N_c=140$) in equilibrium. x is the separation from the center of mass of the cluster. The solid curves are numerical solutions of the time-independent Vlasov equation as described in Sec. VII. The upper limit of the spatial integration is $R^*=2$.

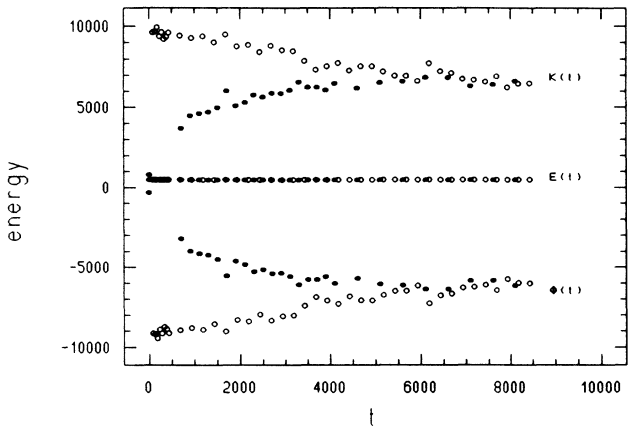

FIG. 9. Total energy E, kinetic energy K, and potential energy Φ for two $N=400$ particle systems as a function of the run time of the simulation. The open circles constitute results of run C1 with an initial configuration chosen such that all particles are concentrated at the same point, $\Phi(t=0)=-79\,800$, and have a kinetic energy $K(t=0)=80\,278$ (both numbers being off the scale of the figure). The cluster shrinks and approaches the equilibrium cluster-particle number from above ($N_c\simeq 142$). The solid circles are the respective results of simulation C3 starting from an equal particle distribution with $\Phi(t=0)=-322$ and a kinetic energy $K(t=0)=800$. This cluster grows and approaches the equilibrium cluster-particle number from below. For both simulations the total energy is about equal, and the same final equilibrium state is obtained.

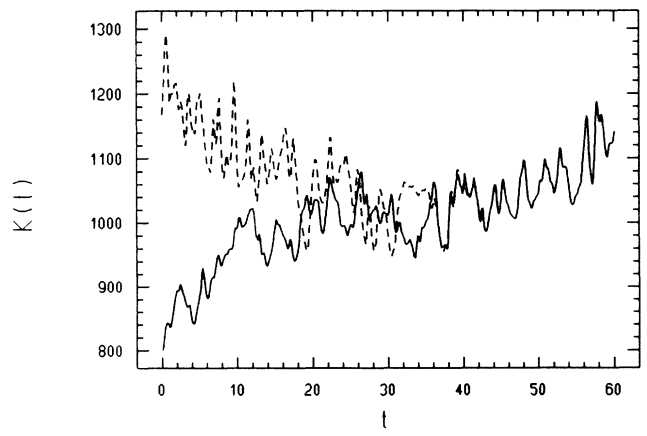

FIG. 10. Total kinetic energy K of a nonequilibrium 400-particle system as a function of the run time for the first 60 time units of the simulation. Starting from an equal particle distribution in V at $t=0$, K starts to rise indicating the growth of a large cluster. At time $t=60$ a time-reversal transformation ($\mathbf{q}\rightarrow\mathbf{q}$, $\mathbf{p}\rightarrow-\mathbf{p}$) is performed and the equations of motion are subsequently integrated backward (dashed line). For 20 time units K is reproduced by the reversed trajectory indicating a shrinking of the cluster. At $t=40$, however, the kinetic energy K starts rising again even in the backward direction indicating the continuation of cluster growth.

arrive at (3.14) and (3.15) the momenta have been rescaled by $\sqrt{N}$ [see (3.7)], whereas no such scaling is performed in the equations of motion used for the simulation. This difference must be corrected for in the following.

To perform the spatial integration in (3.15) a circular volume V^* with radius R^* centered on $\mathbf{R}_c$ is introduced which contains all $N_c(\infty)\equiv N^*$ cluster particles contributing to $n_c^{(1)}(x;N_c)$. Insertion of the potential (2.2a) into (3.15) gives

$$\nu(x)=\beta^*\kappa\int_{V^*}e^{-(\mathbf{x}-\mathbf{y})^2}e^{\nu(y)}d^2y\Big/\int_{V^*}e^{\nu(y)}d^2y\ . \tag{7.7}$$

To arrive at this equation β in (3.15) has to be replaced by $\beta^*=N^*\beta$ to account for the scaling of the momenta mentioned above. Integration over the angle between $\mathbf{x}$ and $\mathbf{y}$ in (7.7) finally yields

$$\nu(x)=\frac{\beta^*\kappa\int_0^{R^*}e^{-(x-y)^2}ye^{\nu(y)}e^{-2xy}I_0(2xy)dy}{\int_0^{R^*}ye^{\nu(y)}dy}\ , \tag{7.8}$$

where I_0 is a modified Bessel function. This nonlinear integral equation may be solved numerically by iteration. Since $\beta^*=N^*/k_BT$, only the equilibrium particle number $N_c(\infty)$ and the equilibrium temperature T are required as input for this computation. The solid lines in Fig. 8 are the result of such a calculation for the respective equilibrium states. The agreement proves that the mean-field theory of Sec. III—identical to the time-independent solution of the Vlasov equation (4.1)—provides a perfect description of the simulation results for the particle density in the equilibrium cluster.

VIII. IRREVERSIBILITY

It has been mentioned before that the approach to equilibrium from the nonequilibrium initial conditions (a) or (b) of Sec. V is extremely slow and requires at least 3×10^6 time steps of duration 0.0025. This slow convergence is demonstrated in Fig. 9 where the kinetic energy $K(t)$, the potential energy $\Phi(t)$, and the total energy E are shown both for a collapsing system [state C3, initial

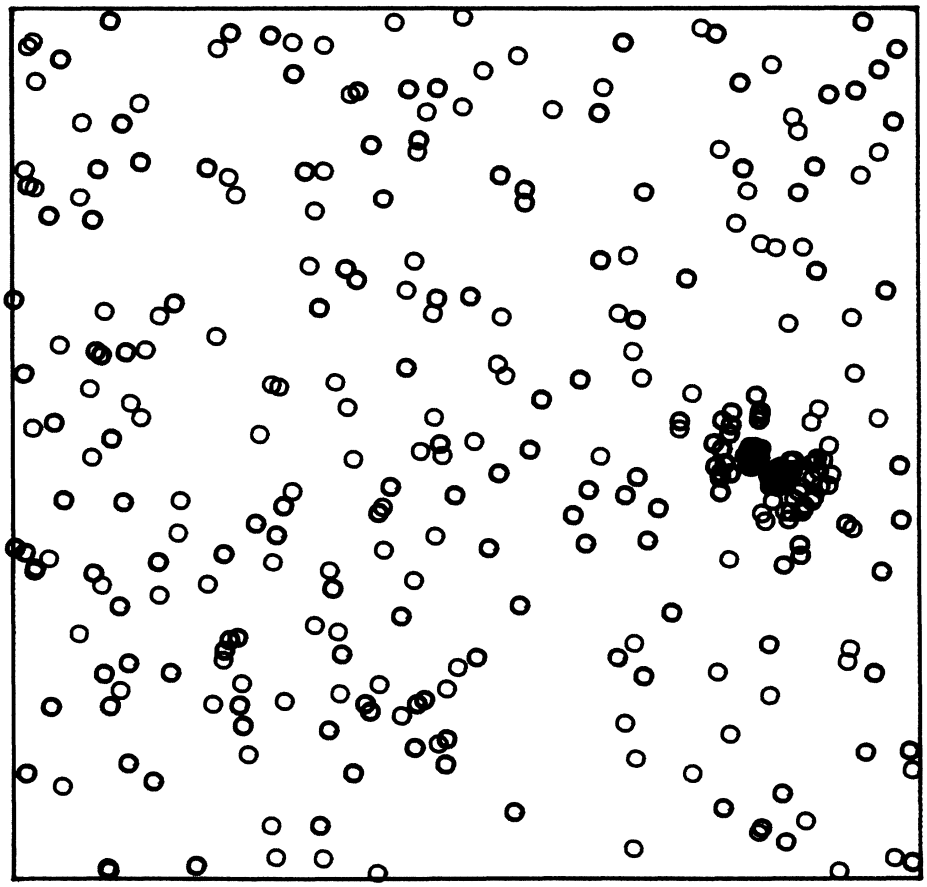

FIG. 11. Equilibrium configuration of system E1 interacting with the electrostatic type of potential (9.1) and (9.2). $N/2=200$ particles carry positive charges (blue), the remaining 200 particles negative charges (red). The formation of a large dipole cluster surrounded by shells of uniformly charged particles is clearly visible. The diameter of the particles in this figure is arbitrary. Its value 0.6 has been chosen to provide a clear display of the structure of the cluster.

condition (a); indicated by solid circles] and a shrinking system [state C4, initial condition (b); open circles]. For both simulations E is about equal and constant in time. The limiting energies are approached only for times $t > 8000$. This indicates weak mixing properties and a much smaller Lyapunov instability than, for example, in Lennard-Jones systems with a repulsive core.[13] To obtain an estimate for the Kolmogorov entropy far from equilibrium we have integrated the equations of motion forward in time for 60 time units starting with the homogeneous initial distribution (a) of run C3. In Fig. 10 the time dependence of the total kinetic energy $K(t)$ is shown by the solid curve. At $t=60$ a time-reversal transformation ($\mathbf{x}\rightarrow\mathbf{x}$, $\mathbf{p}\rightarrow-\mathbf{p}$) is performed and the system subsequently integrated backward (dashed line). For the initial 20 time units of the time-reversed simulation K is indistinguishable from that in the forward direction: the cluster already formed at $t=60$ starts to dissolve when going back. At $t\approx 40$, however, this trend changes and K starts to increase again indicating continuation of cluster growth even in the backward direction. This result is qualitatively independent of the computational accuracy (time step). From two runs with time steps differing by a factor of 2 we estimate that the sum of all positive Lyapunov exponents is of the order of 1. This provides an order-of-magnitude estimate for the Kolmogorov entropy h_K which is equal to the sum of the positive Lyapunov exponent: $h_K \approx 1$. This very small value indicates that any direct measurement of the Lyapunov spectra of such systems is a very tedious procedure.

IX. DISCUSSION

For almost all initial conditions the simulations of model (2.2a) lead to a single dense cluster very early in the run. It floats in the surrounding atmosphere and grows steadily until it reaches its equilibrium size. However, it may happen by accident that two clusters of almost equal particle number $N_{c,1}\approx N_{c,2}$ are formed and compete against each other for further growth. Such a situation has been encountered in one of our simulations and has been recorded on film and videotape.[14] Such metastable states are characterized by a local maximum of the entropy. In finite systems they do not persist very long. When the clusters collide, the global equilibrium characterized by a single cluster is established rather quickly. If $N_{c,1}+N_{c,2}$ before the collision exceeds $N_c(\infty)$ the surplus of clustered particles is evaporated off during the collision process.[14]

The exchange of particles between cluster and surrounding atmosphere is small. This accounts also for the slow convergence rate towards equilibrium. A particle trapped in the cluster oscillates very stably in the mean-field potential experienced in the cluster. This is clearly visible in the film mentioned above.[14]

The choice of potentials of type (2.2a)–(2.2c) for obtaining unstable systems is not unique. It has been mentioned already in the Introduction that a potential of the electrostatic type including attractive and *repulsive* regions may be mechanically unstable. As an example we present results for a system with a Hamiltonian

$$H_N=\sum_{i=1}^{N}\frac{\mathbf{p}_i^2}{2m}+\kappa\sum_{i=1}^{N-1}\sum_{j=i+1}^{N}e_ie_jv(|\mathbf{x}_i-\mathbf{x}_j|)\ , \tag{9.1}$$

where

$$v(x)=x^2e^{-x^2},\quad \kappa=5,\quad |e_i|=1\ . \tag{9.2}$$

Half of the particles carry positive charges ($e_i=1$), the other half negative charges ($e_i=-1$). The equilibrium thermodynamic properties are also given in Table I (state E1). In Fig. 11 a snapshot of an equilibrium configuration is depicted. The positively charged particles (red) and the negatively charged particles (blue) cluster separately in neighboring clusters, in this way forming a large dipole cluster. This simulation demonstrates that charged unstable systems may lead to quite complicated cluster patterns.

ACKNOWLEDGMENTS

The extensive computations were carried out at the computing center of the University of Vienna within the framework of IBM's European Supercomputer Initiative. We gratefully acknowledge the generous allocation of computer time. We thank A. Majerowicz for his help in creating the film mentioned in Ref. 14, and A. Compagner, C. Bruin, and A. Roelse for sending us a copy of their work[1] prior to publication.

[1] A. Compagner, C. Bruin, and A. Roelse, Phys. Rev. A **39**, 5989 (1989).

[2] H. A. Posch, H. Narnhofer, and W. Thirring, in *Simulation of Complex Flows, NATO Advanced Study Institute Series B: Physics,* edited by M. Mareschal (Plenum, New York, in press).

[3] D. Lynden-Bell and R. Wood, Mon. Not. R. Astron. Soc. **138**, 495 (1968).

[4] W. Thirring, Z. Phys. **235**, 339 (1970).

[5] P. Hertel and W. Thirring, Ann. Phys. (N.Y.) **63**, 520 (1971).

[6] H. Jensen (private communications).

[7] P. Hertel and W. Thirring, in *Quanten und Felder,* edited by H. P. Dürr (Vieweg, Braunschweig, 1971), p. 309.

[8] P. Hertel, H. Narnhofer, and W. Thirring, Commun. Math. Phys. **28**, 159 (1972).

[9] E. Hewitt and L. Savage, Trans. Am. Math. Soc. **80**, 470 (1955).

[10] W. Braun and K. Hepp, Commun. Math. Phys. **56**, 101 (1977).

[11] H. Narnhofer and G. L. Sewell, Commun. Math. Phys. **79**, 9 (1981).

[12] W. F. van Gunsteren and H. J. C. Berendsen, Mol. Phys. **34**, 1311 (1977).

[13] H.A. Posch and W. G. Hoover, Phys. Rev. A **38**, 473 (1988).

[14] This film, entitled "Condensation Phenomena in Thermodynamically Unstable Systems: A Simple Two-Dimensional Model for the Formation of Stars," may be obtained from the Österreichisches Bundesinstitut für den Wissenschaftlichen Film, Schönbrunner Strasse 56, A-1050 Vienna, Austria. For a videotaped version one of the authors should be contacted.

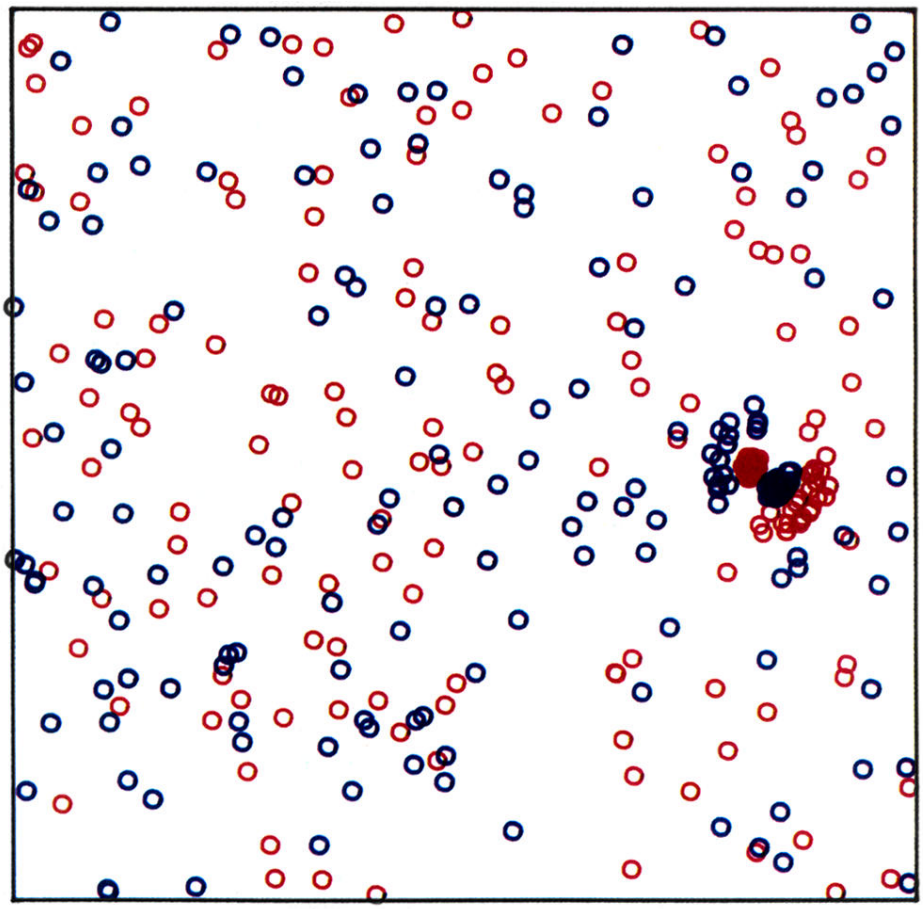

FIG. 11. Equilibrium configuration of system E1 interacting with the electrostatic type of potential (9.1) and (9.2). $N/2=200$ particles carry positive charges (blue), the remaining 200 particles negative charges (red). The formation of a large dipole cluster surrounded by shells of uniformly charged particles is clearly visible. The diameter of the particles in this figure is arbitrary. Its value 0.6 has been chosen to provide a clear display of the structure of the cluster.